Biochemistry (Moscow), Vol. 65, No. 3, 2000, pp. 373-387. Translated from Biokhimiya, Vol. 65, No. 3, 2000, pp. 442-458.

Mechanism of Ca^{2+}-Induced Inhibition of *Escherichia coli* Inorganic Pyrophosphatase

S. M. Avaeva[1]*, N. N. Vorobyeva[2], S. A. Kurilova[1], T. I. Nazarova[1], K. M. Polyakov[3], E. V. Rodina[1], and V. R. Samygina[3]

[1]Belozersky Institute of Physico-Chemical Biology, Lomonosov Moscow State University, Moscow, 119899 Russia; fax: (095) 939-3181; E-mail: avaeva@libro.genebee.msu.su
[2]School of Chemistry, Lomonosov Moscow State University, Moscow, 119899 Russia; fax: (095) 932-8846; E-mail: protein@libro.genebee.msu.su
[3]Shubnikov Institute of Crystallography, Leninskii pr. 59, Moscow, 117333 Russia; fax: (095) 135-1011; E-mail: kostya@ns.crys.ras.ru

Received October 11, 1999

Abstract—The causes of inhibition of *Escherichia coli* inorganic pyrophosphatase (PPase) by Ca^{2+} were investigated. The interactions of several mutant pyrophosphatases with Ca^{2+} in the absence of substrate were analyzed by equilibrium dialysis. The kinetics of Ca^{2+} inhibition of hydrolysis of the substrates $MgPP_i$ and $LaPP_i$ by the native PPase and three mutant enzymes (Asp-42–Asn, Ala, and Glu) were studied. X-Ray data on *E. coli* PPase complexed with Ca^{2+} or $CaPP_i$ solved at atomic resolution were analyzed. It was shown that, in the course of the catalytic reaction, Ca^{2+} replaces Mg^{2+} at the M2 site, which shows higher affinity for Ca^{2+} than for Mg^{2+}. Different properties of these cations account for active site deformation. Our findings indicate that the filling of the M2 site with Ca^{2+} is sufficient for PPase inhibition. This fact proves that Ca^{2+} is incapable of properly activating the H_2O molecule for nucleophilic attack on PP_i. It was also demonstrated that Ca^{2+}, as a constituent of the non-hydrolyzable substrate analog $CaPP_i$, competes with $MgPP_i$ at the M3 binding site. As a result, Ca^{2+} is a powerful inhibitor of all known PPases. Other possible reasons for the inhibitory effect of Ca^{2+} on the enzyme activity are also considered.

Key words: inorganic pyrophosphatase, equilibrium dialysis, Ca^{2+}, inhibition, complex, spatial structure

Soluble inorganic pyrophosphatases catalyze reversible hydrolysis of pyrophosphate (PP_i) to two orthophosphate molecules (P_i) and are the key factors controlling PP_i intracellular level. Pyrophosphate is a product of more than 120 enzymatic reactions. Catalyzing pyrophosphate hydrolysis, pyrophosphatases ensure the synthesis of all vital cellular biopolymers.

Similar to many enzymes involved in phosphate metabolism, PPases are metal-dependent enzymes. Three or four bivalent metal ions are necessary for their catalytic activity; among them, Mg^{2+} is the most powerful effector.

The development of X-ray analysis and PPase synthesis by genetic engineering provided the basis for recent progress in determination of the three-dimensional structures of PPases from *Escherichia coli*, *Saccharomyces cerevisiae*, *Thermus thermophilus*, and *Sulfolobus acidocaldarius*. The crystal structures of the apoenzymes and their complexes, including those with activator metal ions, are presently known [1-5]. These data show that, despite considerable differences in amino acid sequences and subunit structure, PPases from various organisms share similarity in the active site structure and probably in the mechanism of catalysis.

Structure determination of *E. coli* PPase complexes with Mn^{2+} [1] and Mg^{2+} [2, 4] and of *S. cerevisiae* PPase complexes with Mn^{2+} and P_i [3, 5] made it possible to locate the sites responsible for binding of activator metal ions. Figure 1 shows the position of four Mn^{2+} ions at the active site of the PPase subunit [3]. Two sites, M1 and M2, are filled in the absence of substrate; Mg^{2+} and Mn^{2+} bind to these sites similarly [6]. The affinities of M1 and M2 for activator metal ions differ more than tenfold. Thus, for *E. coli* PPase at pH 7.5, K_d (Mg^{2+}) is 50 μM at site M1 and 1.4 mM at site M2 [7]. Two other sites, M3 and M4 (Fig. 1), are occupied with metal cations in enzyme complexes with the substrate or products of the catalytic reaction.

In addition to Mg^{2+} and Mn^{2+}, only Zn^{2+} and Co^{2+} can stimulate pyrophosphate hydrolysis catalyzed by

* To whom correspondence should be addressed.

0006-2979/00/6503-0373$25.00 ©2000 MAIK "Nauka/Interperiodica"

PPases [8]. Ca^{2+}, conversely, is an efficient inhibitor of magnesium pyrophosphate hydrolysis. The enzyme interactions with Ca^{2+}, and inhibition kinetics are best studied for *S. cerevisiae* (baker's yeast) PPase [8-11]. In this instance, inhibition by Ca^{2+} was shown to be due to competition with Mg^{2+} for binding to two binding sites on the enzyme and to a third site on the substrate [10, 12]. In 1983, the structure of yeast PPase complexed with calcium pyrophosphate was reported [13]; however, low resolution (5 Å) allowed the authors to draw only preliminary conclusions concerning Ca^{2+} and $CaPP_i$ binding at the active site.

For *E. coli* PPase, it was demonstrated that Ca^{2+}-induced inhibition is also connected with the replacement of Mg^{2+} from the substrate and from at least one site on the enzyme [14]. Similar results were obtained for all other PPases [15-19]. This suggests that the causes and mode of Ca^{2+} inhibition are common to all PPases. A strong inhibitory effect of Ca^{2+} on PPases may contribute to activity-regulation mechanisms of these constitutive enzymes *in vivo*.

Numerous recent studies have shown that Ca^{2+} is the most common regulator used by living cells from the earliest evolutionary stages [20-22]. The unique properties of Ca^{2+} account for this phenomenon: it is widely spread in nature and capable of rapid and tight binding to proteins; in addition, cells possess a specific system providing quick removal of excess Ca^{2+}. In eucaryotes, Ca^{2+} is involved in regulation of dozens of processes, such as mitosis, muscle contraction, proliferation and differentiation in different types of cells, hormone secretion, etc; it also plays an integrating role controlling coordinated function of different compartments, cells, and organs [22]. Although the utilization of Ca^{2+} in procaryotic cells is not so diverse, it has been shown that Ca^{2+} participates in regulation of such processes as metabolic shift toward the use of a variant food substrate, directional cell movement, etc. [23]. The intracellular Ca^{2+} concentration is normally 10^{-7}-10^{-6} M [19, 20]. Elevated Ca^{2+} concentrations (up to 10^{-5} M) serve as a signal to the cell. At such concentrations, Ca^{2+} produces a strong effect on PPases and other enzymes of phosphate metabolism (kinases, ATPases, and phosphatases [21]). In all probability, this effect forms the basis for the regulatory role of Ca^{2+} in procaryotic cells.

In this work, we investigated the interaction of Ca^{2+} with *E. coli* PPase and some of its mutants both in the absence of substrate and during the catalytic reaction. Such an approach is helpful for the comparison of Ca^{2+} binding sites with those responsible for binding activator metal ions, Mg^{2+} and Mn^{2+}, already located in the PPase three-dimensional structures (Fig. 1).

In collaboration with the staff of the Institute of Crystallography of the Russian Academy of Sciences, we examined the structure of two *E. coli* PPase complexes with Ca^{2+} and calcium pyrophosphate. Their recently solved three-dimensional structures will soon be published. X-Ray data proved useful for understanding the results and, therefore, are used in the discussion.

MATERIALS AND METHODS

The recombinant *E. coli* inorganic pyrophosphatase and mutant enzymes were obtained as described previously [24]. Enzyme suspensions were stored in ammonium sulfate (90% saturation) and desalted on a Sephadex G-50 (fine) column equilibrated with 50 mM Tris-HCl, pH 7.5, before use.

The concentration of pyrophosphatase solutions was determined spectrophotometrically using the absorption value $A^{0.1\%}_{280\ nm}$ of 1.18 [25].

Equilibrium dialysis of inorganic pyrophosphatase and mutants with $^{45}CaCl_2$, and equilibrium dialysis to substitute Ca^{2+} for Mg^{2+} were conducted as described [6].

In this work, we used carrier-free $^{45}CaCl_2$ (Amersham, England) with radioactivity of 0.5-1.0 mCi/ml; Tris, Hepes, $Na_4P_2O_7$, and $CaCl_2$ were from Sigma (USA); $MgCl_2$, $LaCl_3$, and methyl green were from Fluka (Switzerland). In all experiments, titrated $MgCl_2$ and $CaCl_2$ solutions were used; all solutions were prepared using twice-distilled water.

Kinetic measurements. All the measurements were performed in 0.1 M Tris-HCl buffer, pH 7.5. To study $MgPP_i$ hydrolysis, Mg^{2+} and Ca^{2+} concentrations were varied from 0.05 to 2 mM and from 5 to 1500 μM, respectively; $MgPP_i$ concentration was changed from 10 to 120 μM. In the investigations of $LaPP_i$ hydrolysis, Mg^{2+} concentration was 0.6 mM, Ca^{2+} concentration was varied from 5 to 250 μM, and $LaPP_i$ concentration was changed from 20 to 200 μM. $LaPP_i$ was synthesized just before hydrolysis by mixing equimolar amounts of La^{3+} and PP_i; this excluded $CaPP_i$ formation in the reaction mixture. The reaction was initiated by simultaneous addition of Mg^{2+} and the enzyme.

To calculate concentrations, the following K_d values obtained by recalculation of pH-independent values for pH 7.5 were used: 1.29 μM, 2.42 mM, and 126 μM for $MgPP_i$, Mg_2PP_i, and $CaPP_i$, respectively [26]. The concentration of Ca_2PP_i complex was ignored.

Estimation of inhibition parameters. *$MgPP_i$ hydrolysis*. The following scheme for Ca^{2+}-induced inhibition of $MgPP_i$ hydrolysis was suggested:

$$\begin{array}{ccccc}
EMg(1)Ca(2)(MgPP_i) & & EMg_2(MgPP_i) & \rightarrow & \text{products} \\
K'_S \updownarrow & & \updownarrow K_S & & \\
EMg(1)Ca(2) & \overset{K'_2}{\leftrightarrow} & EMg(1) & \overset{K_2}{\leftrightarrow} & EMg_2 \\
K'_C \updownarrow & & \updownarrow K_C & & \\
EMg(1)Ca(2)(CaPP_i) & & EMg_2(CaPP_i) & &
\end{array}$$

Scheme 1

This scheme assumes that $MgPP_i$ and $CaPP_i$ can bind both to EMg_2 and EMgCa. The location of metal cations on the enzyme molecule is shown by figures in parentheses. Thus, EMg(1)Ca(2) is an enzyme subunit with Mg^{2+} at the M1 site and Ca^{2+} at the M2 site.

In Scheme 1, the relationship between $1/v$ and $[CaPP_i]$ (Dixon plot) is as follows:

$$\frac{1}{v} = a + b[CaPP_i] + c[CaPP_i]^2. \quad (1)$$

Coefficients of Eq. (1), a, b, and c, are determined from the following equations:

$$a = \frac{1}{V_0} + \frac{K_S\,(1+\frac{K_2}{[Mg^{2+}]})}{V_0[MgPP_i]}, \quad (2)$$

$$b = \frac{K_S(\frac{1}{K_C} + \frac{zK_SK_2}{K'_S\,K'_2} + \frac{zK_2}{K'_2[MgPP_i]})}{V_0[MgPP_i]}, \quad (3)$$

$$c = \frac{zK_SK_2}{V_0\,K'_2\,K'_C\,[MgPP_i]^2}, \quad (4)$$

where V_0 is the maximum rate of $MgPP_i$ hydrolysis in the absence of inhibitor at saturating substrate concentration; K_2, K'_2, K_S, K'_S, K_C, and K'_C are the constants of the equilibria shown on the Scheme 1; z is the ratio of the dissociation constants of pyrophosphates of calcium and magnesium:

$$z = \frac{K_d(CaPP_i)}{K_d(MgPP_i)}.$$

The ratio of the concentrations of Ca^{2+} and $CaPP_i$ at the fixed concentrations of $[Mg^{2+}]$ and $[MgPP_i]$ is determined by the equation:

$$[CaPP_i] = z[Ca^{2+}]\frac{[MgPP_i]}{[Mg^{2+}]}. \quad (5)$$

Nonlinear regression analysis of the data using Eqs. (1)-(5) allowed us to calculate the parameters V_0, K'_2/K_2, K_S, K'_S, and K'_C. Using K_2 values from 0.5 to 2 mM, K'_2 was estimated. The K_C and K'_S parameters were determined interdependently. The calculations show that, in a wide range of K'_S values, K_C varies not more than 3-5-fold and reach saturation. In Table 2, the limit K_C and corresponding K'_S values for the native PPase and Asp-42–Asn variant are given. For Asp-42–Glu and Asp-42–Ala PPases, only the lower K'_C limit could be determined.

$LaPP_i$ hydrolysis. Scheme 2 was suggested to describe inhibition of $LaPP_i$ hydrolysis by Ca^{2+}:

$$\begin{array}{ccc} & \overset{K'_2}{} & \overset{K_2}{} \\ EMg(1)Ca(2) & \leftrightarrow & EMg(1) \leftrightarrow EMg_2 \\ K'_S \updownarrow & & \updownarrow K_S \\ EMg(1)Ca(2)(LaPP_i) & & EMg_2(LaPP_i) \rightarrow \text{products} \end{array}$$

Scheme 2

According to this scheme, Ca^{2+} inhibits $LaPP_i$ hydrolysis by competition with Mg^{2+} for the M2 binding site. In the absence of Mg^{2+}, PPase does not hydrolyze $LaPP_i$, i.e., the form $ECa_2(LaPP_i)$ is inactive.

It follows from Scheme 2 that under experimental conditions, the dependence of $1/v$ on Ca^{2+} concentration is linear:

$$\frac{1}{v} = a + b[Ca^{2+}]. \quad (6)$$

The coefficients of Eq. (6) are determined from the following equations:

$$a = \frac{1}{V_0} + \frac{K_S}{V_0[LaPP_i]}(1+\frac{K_2}{[Mg^{2+}]}), \quad (7)$$

$$b = \frac{K_SK_2}{V_0[Mg^{2+}]K'_2[LaPP_i]} + \frac{K_SK_2}{V_0K'_2\,K'_S[Mg^{2+}]}, \quad (8)$$

where V_0 is the maximal rate of the $LaPP_i$ hydrolysis in the absence of the inhibitor at the saturating substrate concentration; K_S, K'_S, K_2, and K'_2 are the constants of the equilibria shown on Scheme 2.

Under experimental conditions, the straight lines ($1/v$, $[Ca^{2+}]$) at different $[LaPP_i]$ are virtually parallel (inhibition is formally assigned to the mixed type), so that:

$$b \approx \frac{K_2K_S}{V_0\,K'_2\,K'_S[Mg^{2+}]}. \quad (8a)$$

Data analysis by a nonlinear regression method using Eqs. (6)-(8) allowed us to determine parameters V_0, K_S, and $K'_2K'_S/K_2$ and estimate K'_S. In Table 3, $K'_2K'_S/K_2$ values as well as K'_S and K'_2 parameters are presented. Calculated V_0 values agree well with those obtained from kinetic studies of $LaPP_i$ hydrolysis in the absence of inhibitor.

RESULTS

Ca^{2+} binding in the absence of substrate. In our previous work [6], using equilibrium dialysis we showed that *E. coli* PPase subunit binds two Ca^{2+} cations in the absence of substrate. The form of the curve in Scatchard plot indicates cooperativity of binding (probably between analogous binding sites in different hexamer subunits). One of two Ca^{2+} cations associated with PPase subunit may be replaced by Mg^{2+}. K_d for Mg^{2+} at this site is 0.54 ± 0.07 mM (Table 1); this corresponds to the low-affinity Mg^{2+}-binding site (M2 in Fig. 1).

Earlier, using fluorometric titration, it was shown [8] that a high-affinity Mg^{2+}-binding site (of two sites filled in the absence of substrate) coincides with a low-affinity Ca^{2+}-binding site and *vice versa*.

A similar approach is inapplicable to *E. coli* PPase. To elucidate whether this inversion also takes place in *E. coli* PPase, we analyzed the mutant PPases with substitutions of active site groups responsible for Mg^{2+} binding. Equilibrium dialysis with $^{45}Ca^{2+}$ was conducted with the mutant variants Asp-65–Asn, Asp-67–Asn, Asp-70–Asn, Asp-97–Asn, Asp-102–Asn, Asp-42–Asn, Asp-42–Glu, and Asp-42–Ala, and for some of them, equilibrium dialysis to substitute $^{45}Ca^{2+}$ by Mg^{2+} was performed. The results are shown in Fig. 2 and summarized in Table 1.

The data demonstrate that, of all mutant PPases, the variants Asp-97–Asn, Asp-102–Asn, and Asp-42–Glu retain the ability of the native enzyme (WT) to bind two Ca^{2+} cations per subunit. Under experimental conditions, Asp-65–Asn, Asp-67–Asn, Asp-70–Asn, and Asp-42–Asn PPases bind only one Ca^{2+}, while Asp-42–Ala PPase binds three Ca^{2+} ions.

Analysis of Ca^{2+} substitution for Mg^{2+} shows that all PPases (Asp-65–Asn, Asp-102–Asn, Asp-42–Asn, Asp-42–Glu, and Asp-42–Ala) are similar to WT PPase in their ability to replace one Ca^{2+} by Mg^{2+}. The dissociation constant for Mg^{2+} at this site varies from 0.36 mM for Asp-102–Asn PPase to 2.47 mM for Asp-42–Asn PPase; this corresponds to the low-affinity binding site (M2 in Fig. 1).

The data are consistent with the hypothesis that two Ca^{2+}-binding sites with different affinity for Ca^{2+} are present at the active site of the PPase subunit. It is difficult to estimate Ca^{2+}-binding parameters in WT PPase due to cooperative interactions [6]. In mutant PPases, these sites are filled independently; this makes it possible to determine the dissociation constant for the high-affinity site, which varies from 0.17 mM for Asp-65–Asn PPase to 0.67 mM for the Asp-42–Glu mutant enzyme (Table 1). The dissociation constant for the second Ca^{2+}-binding site cannot be estimated, since under experimental conditions (0.6 mM Ca^{2+}), it is not yet filled.

The mutant Asp-42–Ala PPase has a third Ca^{2+}-binding site, in which the metal may be substituted by Mg^{2+} with K_d = 212 μM.

Table 1. Equilibrium dialysis of the native (WT) and mutant PPases with $^{45}Ca^{2+}$ and Mg^{2+}

Enzyme	$^{45}Ca^{2+}$ binding		Substitution for Mg^{2+}	
	number of sites	K_d, μM*	number of sites	K_d, mM
WT PPase [6]	2	cooperative binding	1	0.54 ± 0.07
Asp-65Asn	1	174 ± 35	1	2.1 ± 1.0
Asp-67Asn	1	153 ± 40	not measured	
Asp-70Asn	1	230 ± 20	not measured	
Asp-97Asn	2	200 ± 20	not measured	
Asp-102Asn	2	210 ± 60	1	0.36 ± 0.07
Asp-42Ala	3	145 ± 20	2	(1)** 0.21 ± 0.03 (2) 0.76 ± 0.20
Asp-42Glu	2	670 ± 350	1	1.3 ± 0.3
Asp-42Asn	1	178 ± 25	1	2.5 ± 0.4

* K_d (Ca^{2+}) values for the high-affinity site are presented, since only this site is saturated under experimental conditions. K_d (Ca^{2+}) for other sites, if any, is estimated with large relative errors and is not shown.

** Dissociation constants for the two sites are given.

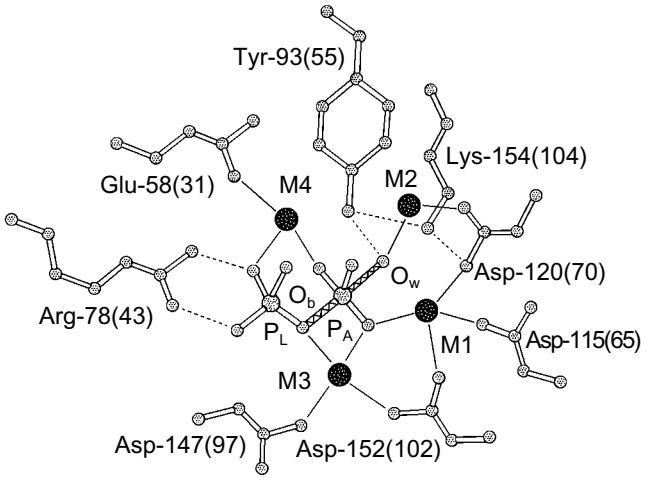

Fig. 1. Presumed transition state at the active site of yeast (*S. cerevisiae*) PPase subunit complexed with Mn^{2+} and P_i [3]. Designations: O_b, bridge-type oxygen atom from pyrophosphate; O_w, attacking water molecule. The positions of corresponding residues in *E. coli* PPase are given in parentheses. Metal ions are shown by black circles. Metal-binding sites are numbered from M1 to M4; the phosphate-binding sites are denoted by P_A and P_L.

Inhibition kinetics of $MgPP_i$ hydrolysis by Ca^{2+}. As it follows from equilibrium dialysis [6], spectrophotometric titration, and *E. coli* PPase protection from proteolysis [7], Ca^{2+} has at least two binding sites on the enzyme. These sites differ in affinity for Ca^{2+}: $K_d(1)$ measured by different procedures varies from 19 to 68 μM, and $K_d(2)$ is 2.5 mM at pH 7.5 [7]. It was suggested that Ca^{2+} binding to one of these sites is involved in inhibition of $MgPP_i$ hydrolysis; one more calcium ion competes with Mg^{2+} for substrate binding [14]. It still remains unclear the filling of which sites leads to inhibition of $MgPP_i$ hydrolysis.

In this work, we explored Ca^{2+} inhibition kinetics of $MgPP_i$ hydrolysis for WT PPase in relation to Mg^{2+}, Ca^{2+}, and $MgPP_i$ concentrations. In Fig. 3a, the relationship between hydrolysis rate and free Mg^{2+} concentration at several constant Ca^{2+} concentrations is shown. The linear dependences in double-reciprocal plots show that, in a given range of Mg^{2+} and Ca^{2+} concentrations, Ca^{2+} competes with Mg^{2+} at only one site. The dissociation constant $K_d(Mg^{2+})$ 0.53 mM calculated at 20 μM Ca^{2+} concentration is in good agreement with the value obtained by equilibrium dialysis to substitute Ca^{2+} for Mg^{2+} (0.54 mM, see Table 1). This value corresponds to the low-affinity Mg^{2+}-binding site (M2 in Fig. 1). The M1 site (high-affinity Mg^{2+}-binding site, $K_d(Mg^{2+})$ 50 μM at pH 7.5 [7]) is filled under experimental conditions. Hence, we showed that Ca^{2+} replaces Mg^{2+} from the M2 site, whose affinity for Ca^{2+} is considerably higher than for Mg^{2+} ($K_d(Ca^{2+})$ determined from the secondary plot is 65 μM; Fig. 3a).

In the absence of Mg^{2+}, *E. coli* PPase does not hydrolyze pyrophosphate even at excessive Ca^{2+} concentrations (up to 10 mM). This means that Ca^{2+} cannot act as an activator, although it is capable of binding to the "activating" M2 site.

Figure 3, b and c, shows the relationship between $MgPP_i$ hydrolysis rate and Ca^{2+} concentration in the presence of 0.6 mM Mg^{2+}. The dependence in ($1/[Ca^{2+}]$, $v/(V_0 - v)$) coordinates (Fig. 3b) allows one to evaluate the degree of inhibition [27]. The fact that the straight line passes through the origin indicates that, in the presence of Mg^{2+}, PPase does not hydrolyze $CaPP_i$ at a detectable rate.

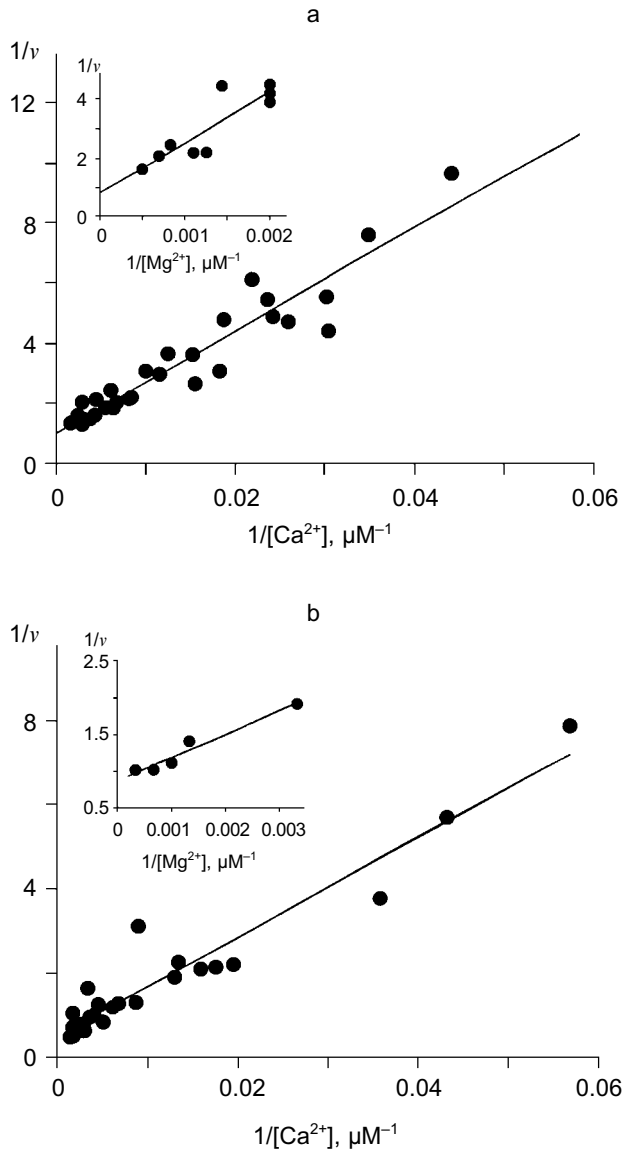

Fig. 2. Equilibrium dialysis of mutant PPases Asp-65–Asn (a) and Asp-102–Asn (b) against $^{45}Ca^{2+}$ (double-reciprocal plot). The results of equilibrium dialysis of these enzymes to substitute $^{45}Ca^{2+}$ by Mg^{2+} are given in insets.

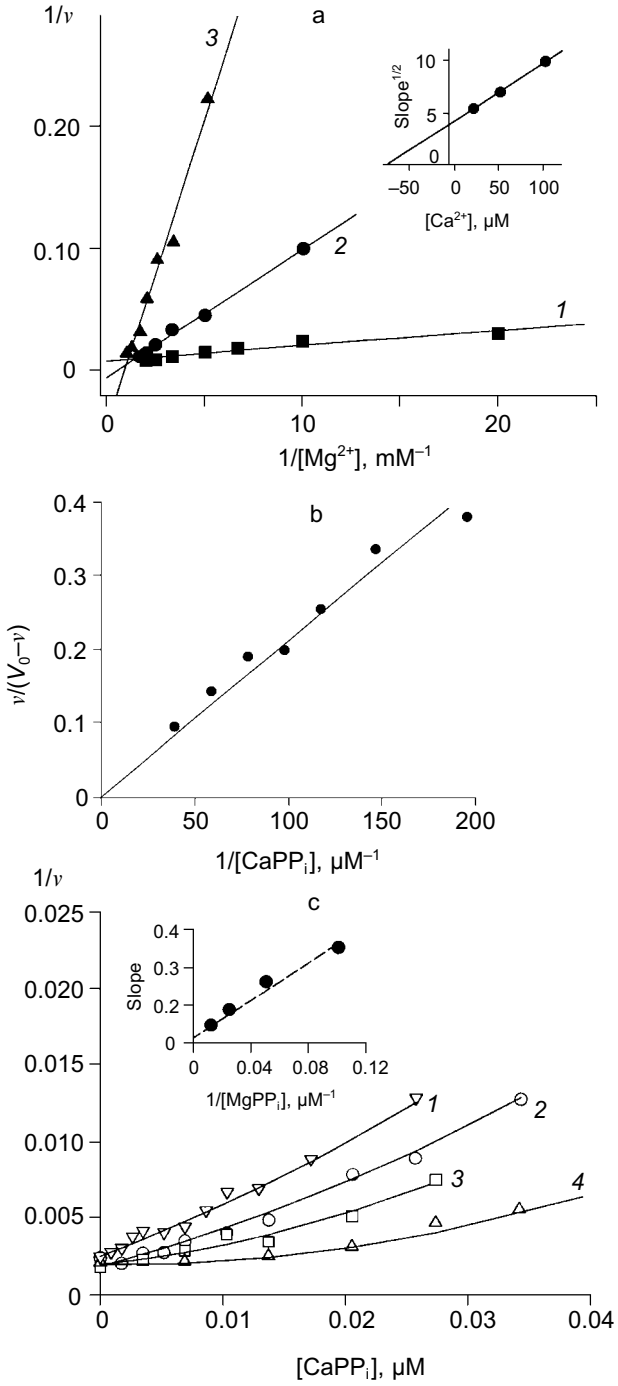

Fig. 3. a) Dependence of $MgPP_i$ hydrolysis rate (v) on Mg^{2+} concentration at constant concentrations of free Ca^{2+} (20 (*1*), 50 (*2*), and 100 μM (*3*)) for WT PPase at pH 7.5 and [$MgPP_i$] of 40 μM. A secondary dependence of the slope of lines on [Ca^{2+}] is given in insets. Here and below the rate of hydrolysis is expressed in international units. b) Dependence of the rate of $MgPP_i$ hydrolysis by WT PPase on $CaPP_i$ concentration. Coordinates are taken from [21] (pH 7.5, [Mg^{2+}] is 0.6 mM, [$MgPP_i$] is 20 μM). c) Inhibition of $MgPP_i$ hydrolysis catalyzed by WT PPase by Ca^{2+} (Dixon plot). Concentration of $MgPP_i$: 10 (*1*), 20 (*2*), 40 (*3*), and 80 μM (*4*). Calculated Hill coefficients: 0.63 (*1*), 0.87 (*2*), 1.16 (*3*), and 1.58 (*4*). A secondary dependence of the initial slope of the curves on 1/[$MgPP_i$] is shown in the inset.

Figure 3c shows Dixon relationships between hydrolysis rate and inhibitor concentration ([I], 1/v). For convenience, to calculate kinetic parameters, $CaPP_i$ concentrations proportional to [Ca^{2+}] at each constant [$MgPP_i$] were plotted on the abscissa instead of free Ca^{2+} concentrations. Figure 3c shows a clear-cut nonlinear dependence of 1/v on [I]. This indicates the involvement of several Ca^{2+} ions in inhibition, which is confirmed by determination of Hill coefficients (given in Fig. 3 legend). Considerable deviation from the straight line indicates the presence of the term $[CaPP_i]^2$ in the expression for 1/v. This means that, under experimental conditions, the forms with two calcium ions ($EMgCaCaPP_i$) participate in inhibition. Based on this finding and the above-mentioned consideration that at 0.6 mM Mg^{2+}, the M1 site is completely filled with Mg^{2+}, an inhibition scheme has been suggested (Scheme 1). It assumes that both $MgPP_i$ and $CaPP_i$ can bind to EMg_2 and EMgCa. In this scheme, the equilibria for binding of free pyrophosphate to EMg_2 and EMg(1)Ca(2) are omitted. The calculations show that the maximum $[PP_i]_{free}$ value under experimental conditions does not exceed 0.2 μM, while K_d of the PP_i complex with any enzyme form is above 100 μM [8]. The combination of Eqs. (1)-(5) gives the equation for the hydrolysis rate (1a) in Dixon coordinates as follows:

$$\frac{1}{v} = \frac{1}{V_0}\left[1 + \frac{K_S}{[MgPP_i]}\left(1 + \frac{K_2}{[Mg^{2+}]}\right)\right] +$$

$$+ \frac{K_S[CaPP_i]}{V_0[MgPP_i]}\left(\frac{1}{K_C} + \frac{zK_SK_2}{K'_SK'_2} + \frac{zK_2}{K'_2[MgPP_i]}\right) +$$

$$+ \frac{K_S[CaPP_i]^2}{V_0[MgPP_i]^2}\cdot\frac{zK_2}{K'_2K'_C}. \qquad (1a)$$

In "Materials and Methods", we showed that Eq. (1a) allows one to evaluate the parameters of Scheme 1. The calculated values are summarized in Table 2. Analysis of these parameters leads to several intriguing conclusions.

1. At the M2 site, as we expected, PPase affinity for Ca^{2+} is higher than for Mg^{2+} ($K'_2/K_2 = 5\cdot10^{-3}$). To estimate K'_2 given in Table 1, K_2 values from 0.53 mM (obtained in the previous kinetic experiment for [Ca^{2+}] of 20 μM, Fig. 3a) to 2.0 mM (determined by UV-spectroscopy [28]) were used. It should be noted that the affinity of this site for metal ions increases in the presence of substrate [29]. This may affect K_2 and K'_2 values measured by kinetic methods.

2. The K'_S value of 10 μM is much higher than K_S = 0.45 μM. This is unexpected, since it is assumed that $MgPP_i$ affinity for Mg^{2+}- or Ca^{2+}-activated enzyme is virtually the same [8, 10]. The same holds for K_C and K'_C parameters. Estimation of K_C shows good agreement

Table 2. Ca^{2+} inhibition parameters of $MgPP_i$ hydrolysis by native and mutant PPases (calculated according to Scheme 1 at pH 7.5 and $[Mg^{2+}]$ of 0.6 mM)

Enzyme	WT PPase	Asp-42Ala	Asp-42Glu	Asp-42Asn
K_2'*, μM	2-12	50-800	15-150	1400-7600
K_S, μM	0.45 ± 0.05	2.0 ± 0.5	10 ± 5	2.0 ± 0.5
K_S'*, μM	10	5	10	2
K_C, μM	$2.4 \cdot 10^{-3}$	$4.5 \cdot 10^{-3}$	$7 \cdot 10^{-3}$	$0.5 \cdot 10^{-3}$
K_C', μM	0.06 ± 0.02	>200	0.09 ± 0.03	>200
V_0**, U	825 ± 5	100 ± 10	40 ± 5	600 ± 50
V_0***, U	1167	103.8	89.4	1728
K_m***, μM	0.13	1.67	9.08	2.00

* Estimated parameters determined interdependently are given (for details see "Materials and Methods"). To estimate K_2', K_2 values from 0.5 to 2 mM were used.
** Calculated according to Scheme 1.
*** pH-Independent values obtained from kinetic studies at $[Mg^{2+}]$ of 5 mM.

with equilibrium dialysis data for yeast PPase, according to which $K_{CaPPi} = 7 \cdot 10^{-9}$ M [8]. However, $CaPP_i$ affinity for EMg(1)Ca(2) (K_C') is significantly lower than the expected value. The reason for this discrepancy is unknown; however, it indicates different effects of Mg^{2+} and Ca^{2+} on the active site conformation.

3. The comparison of K_C and K_S, as well as K_C' and K_S', indicates that the affinity of various PPase forms for Ca^{2+} is several orders of magnitude higher than for Mg^{2+}.

On the whole, the experimental data are well described by Scheme 1. Our results show that Ca^{2+} competes with Mg^{2+} for the M2 site (low-affinity for Mg^{2+} and high-affinity for Ca^{2+}), while $CaPP_i$ competes with $MgPP_i$. All dissociation constants including K_2' do not exceed 10 μM; this accounts for very high effective Ca^{2+} inhibition constants for all known PPases [15-19].

Kinetics of Ca^{2+} inhibition of $LaPP_i$ hydrolysis. The binding constants of pyrophosphate complexes with such cations as Cr^{3+} and La^{3+} are very high (~10^{17} M^{-1} [30]); therefore, we can postulate that Cr^{3+} (La^{3+}) as substrate constituents cannot be replaced either by Mg^{2+} or by Ca^{2+}. (The corresponding dissociation constants for $MgPP_i$ and $CaPP_i$ are given in "Materials and Methods"). In the presence of Mg^{2+}, $CrPP_i$ is hydrolyzed by *E. coli* PPase, although much more less effectively than $MgPP_i$. The inhibition of $CrPP_i$ hydrolysis by Ca^{2+} was earlier used to show that one of the inhibitory Ca^{2+} ions is a substrate constituent [7].

In this work, we investigated Ca^{2+} inhibition of $LaPP_i$ hydrolysis. Under the experimental conditions, free pyrophosphate was absent from the reaction mixture; therefore, $CaPP_i$ was not formed. This allowed us to eliminate the "substrate" Ca^{2+}-binding site and to calculate the inhibition parameters using a simplified model.

Figure 4 shows the results of this part of the work. The relationships between hydrolysis rate and concentrations of Ca^{2+} ((a) Dixon plot) and substrate ((b) Lineweaver–Burk plot) are shown. As we expected, the dependences are linear; this means that one Ca^{2+} ion is sufficient for PPase inhibition. In ($1/[Ca^{2+}]$, $v/(V_0 - v)$) coordinates, all straight lines pass through the origin; this shows that similar to $MgPP_i$ inhibition, $LaPP_i$ inhibition is complete (not shown). The kinetic parameters of $LaPP_i$ hydrolysis at pH 7.5 and $[Mg^{2+}]$ of 0.6 mM in the absence of Ca^{2+} are V_0 = 13.6 U, K_m = 356 μM (Table 3).

The experimental data are most adequately described by Scheme 2. According to this scheme, Ca^{2+} inhibits $LaPP_i$ hydrolysis through competition with Mg^{2+} for the M2 site. In the absence of Mg^{2+}, PPase does not hydrolyze $LaPP_i$, namely, the form $ECa_2(LaPP_i)$ is inactive. Scheme 2 does not take into consideration the formation of this enzyme form, since as mentioned above, at $[Ca^{2+}] < 200$ μM, only one calcium cation is involved in inhibition.

The experimental design was such that all pyrophosphate added to the reaction mixture was in the $LaPP_i$ form. Therefore, Scheme 2 is a simplified variant of Scheme 1. The combination of Eqs. (6)-(8) gives Eq. (6a) for the rate of $LaPP_i$ hydrolysis in Dixon coordinates:

$$\frac{1}{v} = \frac{1}{V_0}\left[1 + \frac{K_S}{[LaPP_i]}\left(1 + \frac{K_2}{[Mg^{2+}]}\right)\right] +$$

$$+ [Ca^{2+}]\ \frac{K_S K_2}{V_0 K_2'[Mg^{2+}][LaPP_i]}\left(1 + \frac{[LaPP_i]}{K_S'}\right), \quad (6a)$$

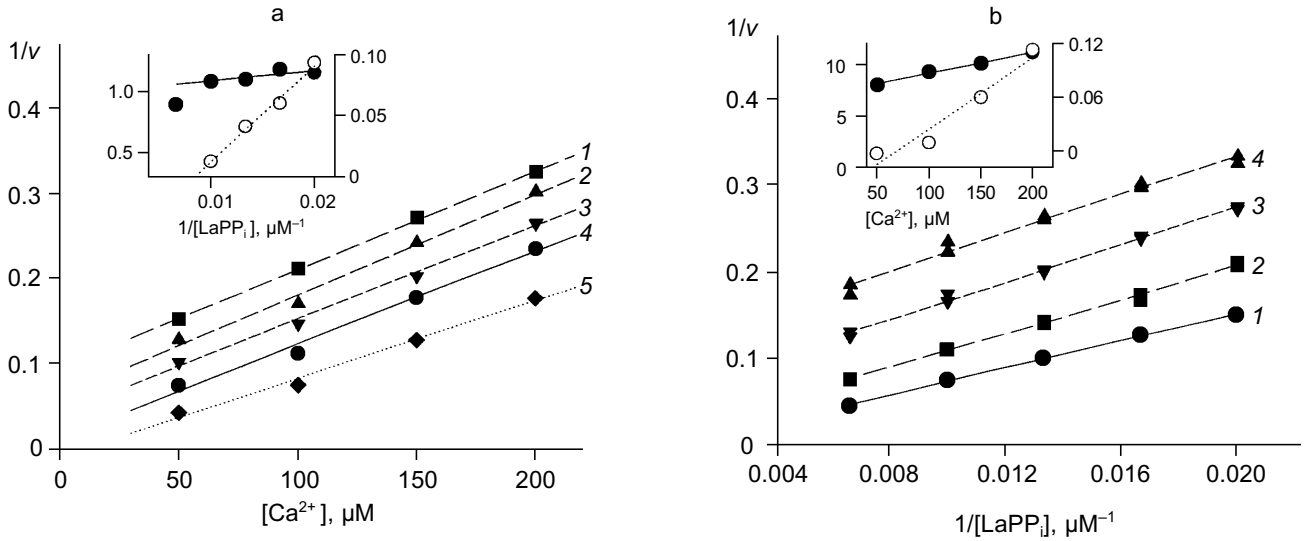

Fig. 4. a) Dependence of the rate of $LaPP_i$ hydrolysis by WT PPase on Ca^{2+} concentration (Dixon plot). $LaPP_i$ concentration: 50 (*1*), 60 (*2*), 75 (*3*), 100 (*4*), and 200 (*5*) μM. b) Dependence of the rate of $LaPP_i$ hydrolysis by WT PPase on $LaPP_i$ concentration (Lineweaver–Burk plot). Ca^{2+} concentration: 50 (*1*), 100 (*2*), 150 (*3*), and 200 μM (*4*). Secondary plots for estimating kinetic parameters are shown in insets (the initial slope of the curves is marked with filled circles, left ordinate; open circles show the intercept on the 1/*v* ordinate, right ordinate).

where V_0 is the maximum rate of $LaPP_i$ hydrolysis in the absence of inhibitor at substrate saturation; other parameters are taken from Scheme 1.

Estimation of inhibition parameters using Scheme 2, gives K_S, K'_S, and K'_2/K_S values. These results together with $LaPP_i$ hydrolysis parameters in the absence of Ca^{2+} (V_0 and K_m) are summarized in Table 3.

The comparison of $MgPP_i$ and $LaPP_i$ hydrolysis parameters leads to the following conclusions.

1. The maximum rate of $LaPP_i$ hydrolysis by the native PPase is two orders of magnitude lower than that of $MgPP_i$. This finding differs from the literature data on hydrolysis of pyrophosphates of lanthanum and other rare-earth elements by yeast PPase [30]. In all likelihood, the active site of *E. coli* PPase is more specific with respect to the substrate metal ion than the active site of the yeast enzyme.

2. The affinity of $LaPP_i$ for EMg_2 is by a factor of 300 weaker than the affinity of $MgPP_i$ for EMg_2. Similar results were obtained with yeast PPase [30]. However, the dissociation constants of $LaPP_i$ and $MgPP_i$ complexes with EMg(1)Ca(2) are at least of the same order. These data indicate that the nature of metal ion at the M2 site is important for optimum conformation of the substrate-binding site.

3. The comparison of K_S and K'_S parameters shows that enzyme affinity for $CaPP_i$ is much higher than for $LaPP_i$. A similar result was obtained with $MgPP_i$.

Table 3. Parameters of Ca^{2+} inhibition of $LaPP_i$ hydrolysis by native and mutant PPases (calculated according to Scheme 2 at pH 7.5 and $[Mg^{2+}]$ of 0.6 mM)

Enzyme	WT PPase	Asp-42Ala	Asp-42Glu	Asp-42Asn
K'_2 K'_S/K_2, μM	0.047 ± 0.005	0.010 ± 0.007	9 ± 1	0.009 ± 0.001
K'_2*, mM	0.005-0.05	>0.07	0.01-0.1	>0.015
K_S, μM	139 ± 8	98 ± 5	100 ± 10	145 ± 25
K'_S*, μM	0.9-9	<0.14	70	<0.6
V_0**, U	13.8 ± 4.6	4.62 ± 0.17	8.28 ± 0.45	3.18 ± 0.22
K_m**, μM	356 ± 16	428 ± 20	362 ± 50	115 ± 17

* Estimated parameters are presented (for details see "Materials and Methods"). To calculate K'_2, K_2 values from 0.5 to 2 mM were used.
** V_0 and K_m were determined from kinetic studies at pH 7.5 and $[Mg^{2+}]$ of 0.6 mM.

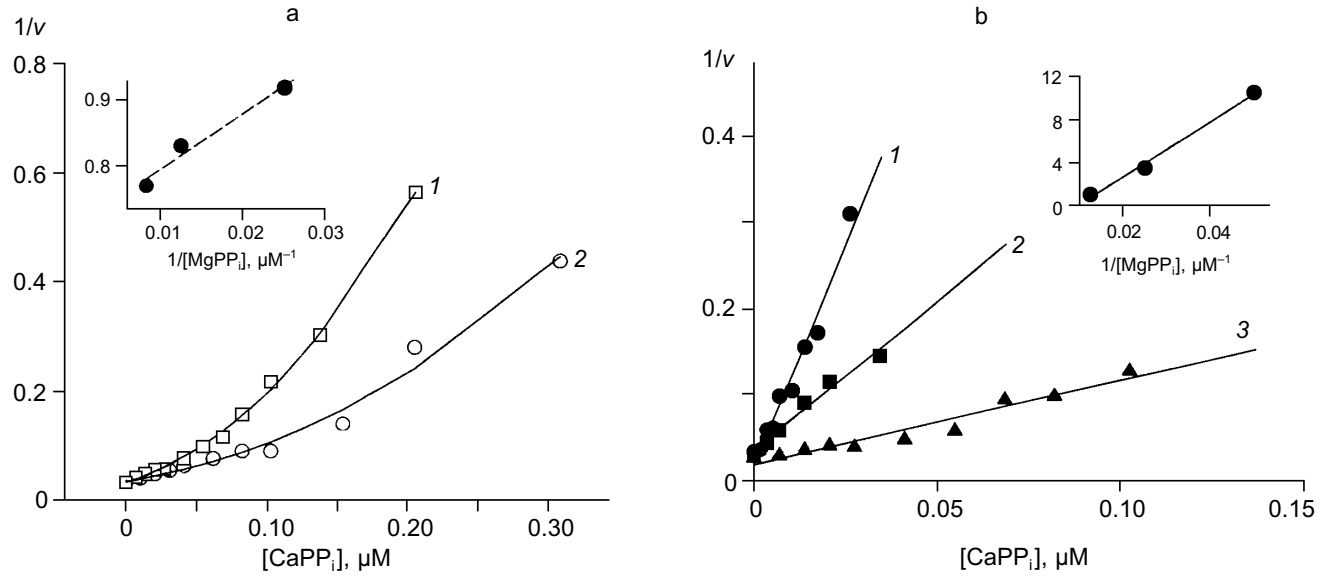

Fig. 5. Dependence of the rate of $MgPP_i$ hydrolysis by mutant PPases on $CaPP_i$ concentration (Dixon plot). a) Asp-42–Glu PPase. $MgPP_i$ concentration: 80 (*1*) and 120 μM (*2*). Calculated Hill coefficients: 1.19 (*1*) and 1.14 (*2*). b) Asp-42–Asn PPase. $MgPP_i$ concentration: 20 (*1*), 40 (*2*), and 80 μM (*3*). Hill coefficient: 0.94 (*1*), 1.04 (*2*), and 1.4 (*3*). Secondary dependences of the initial slope of the curves on 1/[$MgPP_i$] are given in insets.

4. The Ca^{2+} affinity for the M2 site determined from $LaPP_i$ hydrolysis is somewhat lower than the parameter determined from $MgPP_i$ hydrolysis. This probably reflects the effect of substrate on K'_2 and shows that the estimate presented in Table 2 is an effective value.

From these results we may conclude that the filling of M2 site with Ca^{2+} is sufficient for *E. coli* PPase inhibition. If the metal in this site is responsible for activating the attacking nucleophile, this fact unambiguously indicates that Ca^{2+} is ineffective in activating the H_2O molecule.

Ca^{2+} inhibition of mutant PPases with substitutions Asp-42–Ala, Glu, and Asn. It is known that, at concentrations above 5 mM, Mg^{2+} inhibits *E. coli* PPase. According to present views, inhibition is caused by the filling of the fourth metal-binding site (taking into account the substrate site) in the PPase active site. X-Ray data explains inhibition by the filling of the M4 site [3]. The carboxyl group of Glu-31, two oxygen atoms from the substrate, and three water molecules, one of which is coordinated by the side chain of Asp-42, are the metal ion ligands at this site.

To explore whether Ca^{2+} inhibition is connected with the filling of this "inhibitory" site, we studied the behavior of mutant pyrophosphatases with Asp-42 substitutions for Asn, Glu, and Ala under Ca^{2+} inhibition conditions. The conditions for inhibition of $MgPP_i$ and $LaPP_i$ hydrolyses were the same as for WT PPase. Results of the experiments are shown on the Figs. 5 and 6.

Despite different nature of substitutions, all three mutant PPases retained the essential inhibition character-

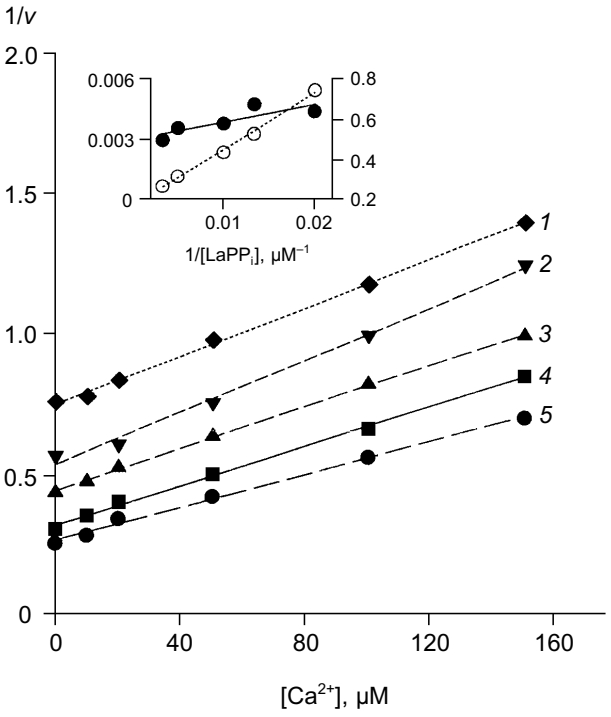

Fig. 6. Dependence of the rate of $LaPP_i$ hydrolysis by Asp-42–Glu PPase on Ca^{2+} concentration (Dixon plot). $LaPP_i$ concentration: 50 (*1*), 75 (*2*), 100 (*3*), 200 (*4*), and 300 μM (*5*). Secondary dependences for estimating kinetic parameters are given in insets (the slope of lines is shown by filled circles, left ordinate; open circles designate the intercept on 1/*v* axis, right ordinate).

istics specific to WT enzyme. Therefore, the experimental data were analyzed using Schemes 1 and 2 for inhibition of $MgPP_i$ and $LaPP_i$ hydrolyses, respectively. Calculated inhibition parameters are given in Tables 2 and 3.

Earlier we studied the kinetics of $MgPP_i$ hydrolysis by three mutant PPases, Asp-42–Asn, Glu, and Ala (the paper is submitted for publication). One of two distinctive features of these mutants, as compared to the native enzyme, consists in high K_m values (see Table 2). The comparison of parameters in Scheme 1 (Table 2) for the native and all mutant PPases shows that this peculiarity is conserved in all three mutants only for $MgPP_i$ binding to EMg_2 (K_S). The K'_S parameters, which characterize $MgPP_i$ binding to EMg(1)Ca(2), and K_C ($CaPP_i$ binding to EMg_2) are virtually the same for all four enzymes. This explains why K'_S and K_S differing by a factor 25 in WT PPase become virtually identical in mutants. This difference shows that, at the active site of the native PPase, there exists an optimum conformation for binding "physiological" ligands, Mg^{2+} and $MgPP_i$, while the substitution of the Asp-42 residue decreases active site specificity with respect to the nature of the associated cation.

In all four enzymes studied, $CaPP_i$ affinity for EMg_2 (K_C) exceeds $MgPP_i$ affinity for EMg_2 (K_S) by several orders of magnitude. Alternatively, Asp-42–Ala and Asp-42–Asn PPases are characterized by worse K'_2 and K'_C parameters (Ca^{2+} affinity for EMg(1) and $CaPP_i$ affinity for EMg(1)Ca(2)).

The inhibition parameters of $LaPP_i$ hydrolysis, as well as V_0 and K_m (Table 3), differ in native and mutant pyrophosphatases to an even lesser extent. Thus, the replacement of Mg^{2+} by La^{3+} leads to elimination of variation in behavior of different enzymes (WT PPase and mutants). This finding supports our suggestion of the existence of an optimum active site conformation and illustrates an important role of the "substrate" metal ion in generating this conformation.

DISCUSSION

Growth and development of a procaryotic cell mainly depend on the nature of a food substrate and energy resources; H^+ (NADH) and organic phosphates (ATP, P_i, and PP_i) are the major regulators of metabolic processes in procaryotes [20]. Since Ca^{2+} affects the enzymes of phosphate metabolism, the changes in intracellular Ca^{2+} and phosphate concentrations are interrelated [31, 32]. The Ca^{2+} ions inhibit PPases at a concentration of ~10^{-5} M; this corresponds to Ca^{2+} maximum level in the cell [20]. In *E. coli*, an increase in PP_i concentration reduces the rate of many processes and finally results in growth inhibition [33]. Accordingly, Ca^{2+}-mediated regulation of pyrophosphatase activity may control PP_i concentration during intracellular signal transduction.

Ca^{2+} binding in the absence of substrate. Our data are consistent with an earlier suggestion that the high-affinity Ca^{2+}-binding site in *E. coli* PPase (K_d measured by different methods varies from 18 to 68 μM [7]) coincides with the low-affinity Mg^{2+}-binding site (K_d = 1.3 mM [22]; M2 in Fig. 1). Equilibrium dialysis of mutant pyrophosphatases also indicates that the low-affinity Ca^{2+} binding site (K_d = 2.0 mM [7]) is located in the region of Asp-65, -67, and -70, namely, it probably coincides with the high-affinity Mg^{2+}-binding site (K_d = 50 μM [7]; M1 in Fig. 1). This conclusion supports the results obtained with WT PPase. Consequently, in *E. coli* PPase, affinity inversion, shown by different methods for yeast PPase, is also observed [8, 11, 12, 28].

The question arises as to why during equilibrium dialysis Mg^{2+} can replace Ca^{2+} from the M2 site, while it does not replace Ca^{2+} from the M1 site, although its affinity for this site is two orders of magnitude higher. This may be due to different properties of Ca^{2+} and Mg^{2+}. The size of a non-hydrated Ca^{2+} ion is much greater than that of Mg^{2+} (their ionic radii are 0.96 and 0.65 Å, respectively [34, 35]). However, a hydrated Ca^{2+} cation is smaller than a hydrated Mg^{2+} cation [36]. Metal binding at the M2 site replaces only one solvent molecule in its coordination sphere (by the oxygen atom of Asp-70 carboxyl group). Therefore, the hydration level of the central ion changes insignificantly resulting in easy mutual substitutions at the M2 site, which depend only on $[Ca^{2+}]/[Mg^{2+}]$ ratio. A different picture is observed at the M1 site. During the filling of this site, the metal ion loses three molecules of the solvent and acquires three protein ligands instead (Fig. 1). In this instance, the size of the central ion becomes very important, and the geometry of the M1 site with associated Ca^{2+} or Mg^{2+} may differ considerably.

The presence of the third Ca^{2+}-binding site in Asp-42–Ala PPase deserves special attention. The mechanism of binding an additional Ca^{2+} may be as follows. The Asp-42 residue in the native PPase is hydrogen-bonded to Glu-31 and forms an ion pair with Lys-29. It seems most probable that the substitution of this residue by hydrophobic alanine releases both ligands. The carboxyl groups of Glu-31 and Glu-20 located in this region form a negatively charged cluster capable of Ca^{2+} binding. Therefore, an additional Ca^{2+} binding site in Asp-42–Ala PPase is probably located in the same region as the site responsible for binding "inhibitory" Mg^{2+} ion (M4 in Fig. 1).

Kinetics of Ca^{2+} inhibition. The kinetic data demonstrate that first, Ca^{2+} is incapable of activating *E. coli* PPase even if it is bound at the "activator" M1 and M2 sites; second, $CaPP_i$ is not hydrolyzed by *E. coli* PPase in the absence of Mg^{2+} and at Mg^{2+} concentrations below 0.6 mM.

Similar results were obtained with yeast PPase. Of more than 15 metals tested, only 3 were able to activate the

enzyme by more than 0.1% compared to Mg^{2+} [10]. Ca^{2+} is not among them. Some cations (La^{3+} and other rare-earth elements) cannot activate the enzyme, although in the presence of a suitable effector, the substrate containing these cations may be hydrolyzed [10, 30]. The available data indicate that the substrate-binding site imposes heavier demands on the nature of the metal ion than the activator site [10]. It was also shown for yeast enzyme that the nature of the substrate metal affects considerably substrate binding and significantly less influences the rate of pyrophosphate hydrolysis [30]. Our findings are in conflict with these data; this is probably another manifestation of the dissimilarity between yeast and *E. coli* PPases.

Ca^{2+} also inhibits PPase-catalyzed ^{18}O exchange between phosphate and water [10].

Estimation of the rate constants for the elementary stages of the yeast PPase-catalyzed reaction in the presence of Mn^{2+}, Zn^{2+}, and Co^{2+} shows that low efficiency of these cations as activators of pyrophosphate hydrolysis is mainly due to a decreased rate of release of hydrolysis products [36]. The inhibition of *E. coli* PPase by excess Mg^{2+} is also associated with this phenomenon [37].

Data analysis allowed us to determine the role of Ca^{2+} at different stages of $MgPP_i$ hydrolysis and suggest the possible causes of its inhibitory effect.

1. The release of hydrolysis products and pyrophosphate hydrolysis are the rate-limiting stages for *E. coli* PPase [36]; therefore, we shall consider them first. The release of pyrophosphate hydrolysis products is probably more complicated in the presence of Ca^{2+} than of Mg^{2+}. First, as was shown for yeast PPase, this is observed with many cations including Mn^{2+}, Zn^{2+}, and Co^{2+}. They bind stronger to the enzyme active site than Mg^{2+} that may interfere with the release of the reaction products. At the same time, the maximum rate of pyrophosphate hydrolysis activated by these cations differs insignificantly, as compared to Mg^{2+}, and is even higher with Zn^{2+} [36]. Second, as we showed in this work, *E. coli* pyrophosphatases bind $CaPP_i$ several orders of magnitude stronger than $MgPP_i$. It probably holds true for calcium and magnesium phosphates. Analysis of the low-molecular-weight compounds of calcium and magnesium demonstrates that Ca^{2+} exhibits higher affinity for carboxylates than Mg^{2+} [23]. We may suppose that this is one of the main factors responsible for stronger binding of Ca^{2+} than of Mg^{2+} to the PPase molecule. Accordingly, more difficult release of the reaction products may account for Ca^{2+} inhibition of PPases.

The kinetics demonstrate that $CaPP_i$ is not hydrolyzed by PPase. However, we cannot rule out that a single $CaPP_i$ hydrolysis act, in which the reaction products remain tightly associated with the enzyme, occurs at the PPase active site in the presence of Mg^{2+}. This makes further hydrolysis of $CaPP_i$ impossible. Thus, the role of Ca^{2+} in the release of the reaction products is still unclear, since these two possibilities are experimentally indistinguishable.

2. Ca^{2+} can occupy the M1 site. The role of the activator metal at the M1 site consists in conformational rearrangements of the active site for catalytically effective substrate binding. Figure 1 shows that one Mn^{2+} ligand at the M1 site (Asp-102 carboxyl group) is simultaneously a metal ligand at the M3 "substrate" site. From the above-mentioned considerations it follows that the mode of Ca^{2+} and Mg^{2+} binding at the M1 site is different. Even if the ligands for these cations at M1 are similar, their relative position, the distance between them and other active site groups, etc., may vary. This variation must inevitably interfere with substrate binding ($MgPP_i$, $CaPP_i$, or $LaPP_i$). However, this hypothesis is not substantiated by the kinetic data, since under experimental conditions, the M1 site is completely occupied by Mg^{2+}.

3. The substrate metal cation screens pyrophosphate charge, thus providing necessary electrophilicity to the attacked phosphorus atom. The efficiency of the metal ion in this instance is determined by its polarizing effect. The calculated polarizing effect of Ca^{2+} is lower than that of Mg^{2+}. This suggestion was confirmed by the study of the effect of Ca^{2+} and Mg^{2+} on H–O–H angle in liganded water molecules and calculated dehydration energies for Ca^{2+} and Mg^{2+} aqua-complexes [38]. However, this problem is more complicated than it may seem. Calcium ions in solution form complexes with a coordination number of 6 or 7 with easy transitions between them. The parameters of Ca^{2+} binding in these complexes and hence, the polarizing effect of the central ion are different. If we compare Ca^{2+} and Mg^{2+} complexes with identical coordination numbers, for example hexahydrates, the effective metal ion charge in these complexes will be 1.57 and 1.18 for Ca^{2+} and Mg^{2+}, respectively [38]. Accordingly, in some instances, the polarizing effect of Ca^{2+} may be comparable or even higher than that of Mg^{2+}. Thus, the activating effects of Ca^{2+} and Mg^{2+} on pyrophosphate are still incompletely understood.

The data on $LaPP_i$ hydrolysis indicate that the nature of metal cation at the M3 site is essential for hydrolysis. The k_{cat} value for $LaPP_i$ hydrolysis by WT PPase is two orders of magnitude lower than for $MgPP_i$ hydrolysis, despite higher La^{3+} charge. It follows from this observation that the functions of the substrate metal cation are not limited to shielding of the pyrophosphate charge. Nevertheless, La^{3+} is capable of substrate activation. In all probability, despite a larger radius as compared to Mg^{2+} (1.06 Å [35]), La^{3+} produces a rather strong polarizing effect due to its higher charge.

4. The role of Ca^{2+} associated at the M2 site is of particular interest. A current model for the mechanism of PPase hydrolytic action suggests that the metal ion at the M2 site functions as a nucleophile activator for the attack on pyrophosphate [3]. Ca^{2+} and Mg^{2+} show different efficiency in activating a water molecule. Thus, the pK_a of the water molecule included in the coordination sphere of the metal ion is 12.9 for Ca^{2+} and 11.4 for

Mg^{2+} [34, 35]. This means that under identical conditions, the concentrations of active nucleophile may differ more than tenfold in these two instances. In addition, calcium cation, which differs in size from Mg^{2+}, may destroy the native conformation of the M2 site affecting the position of metal ligands. At the same time, the orientation of the attacking nucleophile is extremely important for S_N2 reaction efficiency.

As we showed above, Ca^{2+} inhibits $LaPP_i$ hydrolysis under the conditions when $CaPP_i$ is not formed and the concentrations of free Ca^{2+} correspond to complete filling of the M2 site. This fact clearly indicates that Ca^{2+} at the M2 site is incapable of nucleophile activation.

Different effects of Ca^{2+} and Mg^{2+} on the conformation of the M2 binding site were demonstrated earlier by another example. The fluoride ion is a powerful inhibitor of yeast and *E. coli* PPases. It was shown for yeast PPase that F^- binds to the enzyme or enzyme–substrate complex, and irreversible isomerization of the product occurs. Yeast PPase can bind F^- only in the presence of Mg^{2+}, at its concentrations providing complete filling of the M2 site. The resulting enzyme–substrate–magnesium–fluoride complex (E–S–Mg–F) can be isolated by gel-filtration. At the same time, in the presence of Ca^{2+}, the enzyme–substrate complex loses its ability for binding F^- [39].

As will be shown below, the X-ray data are consistent with our conclusions on the effect of Ca^{2+} on the active site conformation.

X-Ray analysis of pyrophosphatase complexed with Ca^{2+} and $CaPP_i$. The structures of *E. coli* PPase complexed with Ca^{2+} and $CaPP_i$ have been solved and refined quite recently. The publication of these results is now in progress. They confirm the experimental findings described above, so we present here only a short description of these data.

The structure of *E. coli* PPase complexed with Ca^{2+} was solved at 1.1 Å resolution. Each enzyme subunit in the complex contains two metal cations at the active site. Their position is shown in Fig. 7. The carboxyl groups of Asp-65, -70, and -102 and three water molecules are Ca^{2+} ligands at one site. The Asp-102 carboxyl group is coordinated with Ca^{2+} in a bidentate manner. The occupancy of this site is 0.8. At the second site, Ca^{2+} ligands are the Asp-70 carboxyl group and six water molecules; the occupancy of this site is 0.7. Therefore, the positions of calcium ions are similar to those at the M1 and M2 sites in Fig. 1. However, both Ca^{2+} ions in the structure under consideration have a coordination number of 7, but not of 6, as Mg^{2+} and Mn^{2+}. This is often observed in proteins and reflects variant properties of these cations.

The structure of the pyrophosphatase–$CaPP_i$ complex was solved at 1.2 Å resolution. In this structure, all six subunits are identical. Each subunit contains two Ca^{2+} ions and $CaPP_i$ at the active site (Fig. 8). Metal ions are associated with the sites analogous to M1, M2, and M3. Ca^{2+} ligands at the M3 site are the carboxyl groups from Asp-97 and Asp-102, two water molecules, and two oxygen atoms from pyrophosphate. It is apparent that Ca^{2+} binds at the M3 site as a substrate constituent; this fact agrees with the order of filling of Mg^{2+}-binding sites proposed earlier [3].

The structural comparison of the M1 and M2 sites of the two PPase complexes reveals several characteristic features. First, the position of Ca^{2+} at the M1 site differs

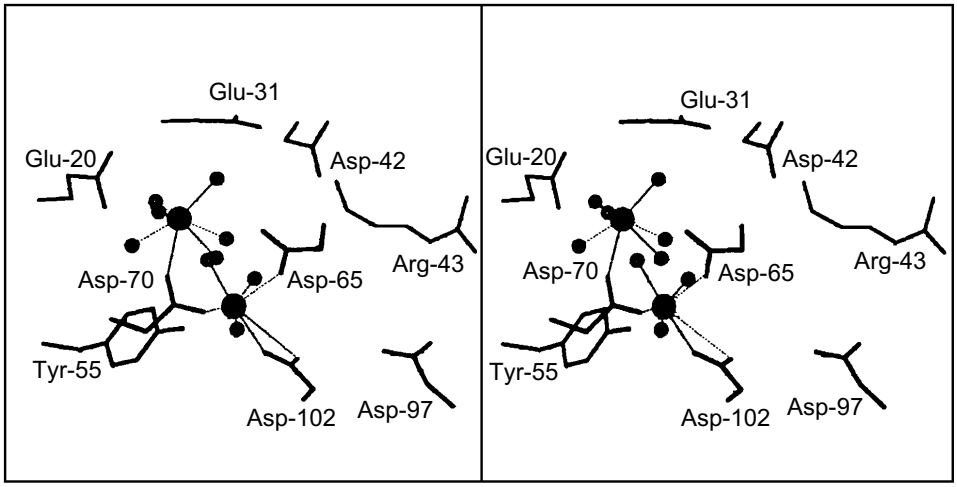

Fig. 7. Active site of *E. coli* PPase complexed with Ca^{2+}. The side groups of the most important residues are shown. Designations: large circles, metal ions; small circles, water molecules (Ca^{2+} ligands). Calcium cations are connected with the ligands by dotted lines. Figures 7 and 8 were generated using the MOLSCRIPT program [42].

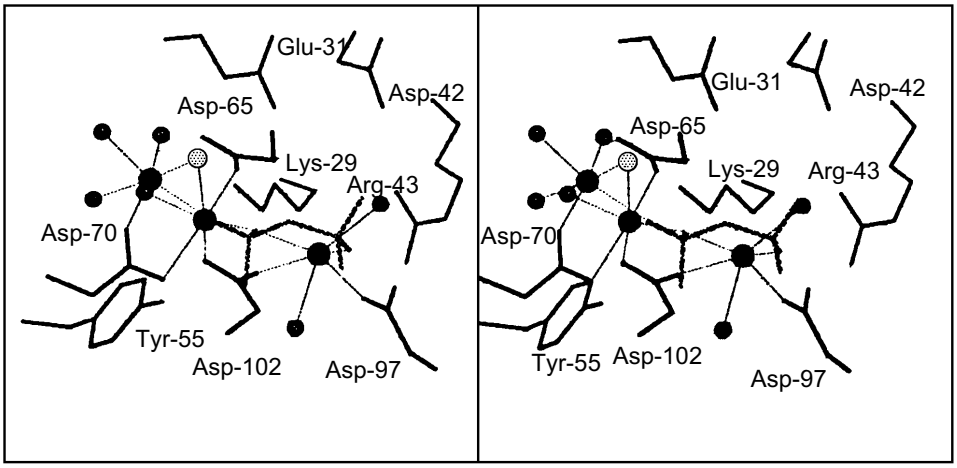

Fig. 8. Active site of the *E. coli* PPase with $CaPP_i$. Metal ions are designated with large filled circles, and water molecules with small filled circles. The bridge-type H_2O molecule linking Ca^{2+} ions is shown as a small gray circle. Pyrophosphate is given in gray color.

considerably: in the $CaPP_i$ complex, it is shifted by 2.39 Å toward pyrophosphate. At this site, the flexible loops of the polypeptide chain (64-70 and 96-102) with Ca^{2+} ligands are significantly displaced. The conformation of the M2 site remains virtually unaffected. The position of Ca^{2+} in these structures differs by 0.8 Å. In the complex with $CaPP_i$, the metal cation at this site has a coordination number of 6, not 7 as in the complex with Ca^{2+}. This results in different arrangement of H_2O molecules, the metal ion ligands (the maximum shift Δ is 0.87 Å). Similar to the M1 site, the substrate oxygen atom becomes Ca^{2+} ligand at M2 instead of one water molecule.

Another interesting structural peculiarity of $CaPP_i$ complex is that at the M1 and M2 sites, two metal ions are bound to one more common ligand, a bridge-type water molecule, in addition to the Asp-70 carboxyl group. This molecule is absent from the Ca^{2+} complex. In all probability, upon substrate binding, one metal ion moves closer to the second ion (3.3 Å), and one of their ligands becomes common to both of them. Similar shifts of Mn^{2+} ions accompanied by the appearance of a common ligand in the presence of two phosphates were described for yeast PPase [5].

To elucidate the mechanism of catalytic reaction, it is interesting to investigate the arrangement of water molecules relative to $CaPP_i$, which is a non-hydrolyzable analog of the substrate. According to the current concept of PPase catalytic action, two different water molecules are supposed to act as attacking nucleophiles. However, analysis of PPase complexed with Ca^{2+} and $CaPP_i$ demonstrates that neither H_2O molecule is located on line to the bridge-type oxygen atom and rather close to phosphorus atoms. Harutyunyan [2, 3] suggested that the attacking water molecule in the PPase complex with the reaction products is replaced by the oxygen atom from one of the phosphates (O_w in Fig. 1). In the complex with non-hydrolyzable $CaPP_i$, the corresponding H_2O molecule is replaced by oxygen from pyrophosphate. According to Cooperman's theory [4, 5], the hydroxyl ion generated from the bridge-type water molecule between metal ions at the M1 and M2 sites is an attacking nucleophile. The bridge-type H_2O molecule linking two Ca^{2+} ions (shown in gray in Fig. 8) is 3.48 Å apart from the nearest phosphorus atom, and upon nucleophilic attack, the angle would be 113 instead of 180°. In addition, only one H_2O molecule at the active site of PPase complexed with $CaPP_i$ is located at a distance, which does not exceed 3.5 Å from the phosphorus atoms; however, it is distant from all three metal cations. The amino group of Lys-148 is its only protein ligand. Thus, neither water molecule can be definitely identified as an attacking nucleophile.

The absence of a specifically oriented water molecule may be connected with different properties of Ca^{2+} and Mg^{2+} leading to divergent conformation of the active site. Superimposing the structure of PPase complexed with Ca^{2+} on the structure of the enzyme–Mg^{2+} complex [2] shows that the positions of metal ions and their ligands changed. As we expected, Ca^{2+} and Mg^{2+} shifted most relative each other at the M1 site (Δ is 1.37 Å). The picture is different for the M2 site: the metal ions are located similarly (Δ is 0.2 Å), although water molecules are displaced by 0.5-0.6 Å. However, even in the structure of the enzyme complexed with Mg^{2+}, it is impossible to find a H_2O molecule located on line with the oxygen atom of calcium pyrophosphate.

Another possible explanation presumes different binding of the substrate at the PPase active site in the presence of various cations. Some kinetic data support this suggestion [36]. Structure investigations of calcium and magnesium pyrophosphates also reveal variation in

conformation of these substrates [40]. Superposition of the structures of PPase complexed with $CaPP_i$ and yeast PPase complexes with the reaction products (and with Mn^{2+} as effector [3, 5]) shows that they hardly differ in the mode of substrate binding. Thus, phosphorus atoms are displaced in these structures by 0.99 and 1.38 Å and the straight line P–P shifts by less than 10°. These differences are most likely due to the movement of phosphate groups induced by hydrolysis. Nevertheless, structural analysis of several mutant PPases demonstrates that even relatively small conformational changes may considerably decrease enzymatic activity [41].

We may also suggest the following explanation. The enzymatic reaction of PP_i hydrolysis/synthesis represents a sequence of many elementary stages. The available models of PPase catalytic action [3, 5] do not take into consideration the complexity of this process. In particular, both presently available structures of yeast PPase–phosphate complex do not explain the mechanism of PP_i synthesis. Two reactions (hydrolysis and synthesis) catalyzed by the enzyme proceed several times during one catalytic act; therefore, it seems reasonable to suggest that after hydrolysis the phosphate groups move relative to each other insignificantly. However, in both instances, the positions of phosphates differed from the expected ones, namely, not a single oxygen atom was in proper orientation for nucleophilic attack on phosphorus. This finding shows that the structural data deals with specific conformation of the active site fixed at an elementary stage following hydrolysis.

The complexity of the processes that occur at the active site during hydrolysis is illustrated by one more observation. As we already noted, in the structure of *E. coli* PPase complexed with $CaPP_i$, each metal ion at the M1 and M2 sites is associated with only one oxygen from phosphate. Since in this complex hydrolysis did not take place, it means that, upon binding to the active site, the substrate replaces one water molecule from the coordination spheres of each of these ions. If the phosphorus atom of pyrophosphate is attacked by the water molecule included in the coordination sphere of the metal ion, an additional contact of this ion with the phosphate formed should appear. However, in both structures of yeast PPase complexed with hydrolysis products [3, 5], each Mn^{2+} preserves a contact only with one oxygen atom from phosphate both at the M1 and M2 sites. This may indicate movement of oxygen atoms due to the turn of the phosphate residue after hydrolysis and loss of the contact with Mn^{2+}. A changed position of phosphate was detected upon the comparison of structures of the yeast mutant Arg-78–Lys PPase complexed with phosphate and WT PPase complexed with phosphates and Mn^{2+} [29]. This fact proves that both structures of PPase complexes with hydrolysis products [3, 5] do not reflect the state of the active site immediately after hydrolysis, but only a subsequent stage of substrate conversion.

In summary, X-ray data are consistent with our hypothesis based on Ca^{2+} inhibition kinetics of *E. coli* PPase: inhibition is mainly due to the distortion of the active site conformation resulting in inability of the enzyme to activate and orient a nucleophile for the attack on pyrophosphate.

In this work we analyzed in detail Ca^{2+}-induced inhibition of *E. coli* PPase. Kinetic studies, equilibrium dialysis of mutant PPases, and X-ray data reveal reasons for the strong inhibitory effect of Ca^{2+} on PPase. First, in the course of catalysis, Ca^{2+} replaces Mg^{2+} from the M2 site, which shows higher affinity for Ca^{2+} than for Mg^{2+}. This results in inability of the enzyme to acquire the optimum for hydrolysis active site conformation and orientation of the attacking nucleophile. In addition, Ca^{2+} is incapable of activating thee H_2O molecule for the attack. Second, we have shown that the nature of the metal cation at the substrate-binding site and its ability to activate the electrophilic phosphorus atom are important for hydrolysis. Third, it has been suggested that, upon catalysis in the presence of Ca^{2+}, the release of hydrolysis products will be affected. These are the reasons for Ca^{2+} being a powerful inhibitor of all known PPases.

This work was supported in part by the Russian Foundation for Basic Research (grants No. 97-04-50031 and No. 96-15-97969) and the "Universities of Russia" program (basic investigations, grant No. 5077).

REFERENCES

1. Harutyunyan, E. H., Oganessyan, V. Yu., Oganessyan, N. N., Terzyan, S. S., Popov, A. N., Rubinskiy, S. V., Vainshtein, B. K., Nazarova, T. I., Kurilova, S. A., Vorobyeva, N. N., and Avaeva, S. M. (1996) *Kristallografiya*, **41**, 84-96.
2. Harutyunyan, E. H., Oganessyan, V. Yu., Oganessyan, N. N., Avaeva, S. M., Nazarova, T. I., Vorobyeva, N. N., Kurilova, S. A., Huber, R., and Mather, T. (1997) *Biochemistry*, **36**, 7754-7760.
3. Harutyunyan, E. H., Kuranova, I. P., Vainshtein, B. K., Höhne, W. E., Lamzin, V. S., Dauter, Z., Teplyakov, A. V., and Wilson, K. S. (1996) *Eur. J. Biochem.*, **239**, 220-228.
4. Kankare, J., Salminen, T., Lahti, R., Cooperman, B. S., Baykov, A. A., and Goldman, A. (1996) *Biochemistry*, **35**, 4670-4677.
5. Heikinheimo, P., Lehtonen, J., Baykov, A., Lahti, R., Cooperman, B. S., and Goldman, A. (1996) *Structure*, **4**, 1491-1508.
6. Avaeva, S. M., Rodina, E. V., Vorobyeva, N. N., Kurilova, S. A., Nazarova, T. I., Sklyankina, V. A., Oganessyan, V. Yu., and Harutyunyan, E. H. (1998) *Biochemistry (Moscow)*, **63**, 592-707.
7. Kurilova, S. A., Bogdanova, A. V., Nazarova, T. I., and Avaeva, S. M. (1984) *Bioorg. Khim.*, **10**, 1153-1160.
8. Ridlington, J. W., and Butler, L. G. (1972) *J. Biol. Chem.*, **247**, 7303-7307.

9. Moe, O. A., and Butler, L. G. (1972) *J. Biol. Chem.*, **247**, 7315-7319.
10. Butler, L. G., and Sperow, J. W. (1977) *Bioinorg. Chem.*, **7**, 141-150.
11. Rapoport, T. A., Höhne, W. E., Heitmann, P., and Rapoport, S. (1973) *Eur. J. Biochem.*, **33**, 341-347.
12. Braga, E. A., and Avaeva, S. M. (1972) *FEBS Lett.*, **27**, 251-255.
13. Kuranova, I. P., Terzyan, S. S., Voronova, A. A., Smirnova, E. A., Vainshtein, B. K., Höhne, W., and Hansen, G. (1983) *Bioorg. Khim.*, **9**, 1611-1619.
14. Kurilova, S. A., Nazarova, T. I., and Avaeva, S. M. (1983) *Bioorg. Khim.*, **9**, 1032-1039.
15. Fraichard, A., Trossat, C., Perotti, E., and Pugin, A. (1996) *Biochimie*, **78**, 259-266.
16. Volk, S. E., Baykov, A. A., Duzhenko, V. S., and Avaeva, S. M. (1982) *Eur. J. Biochem.*, **125**, 215-220.
17. Maeshima, M. (1991) *Eur. J. Biochem.*, **196**, 11-17.
18. Davidson, A. M., and Halestrap, A. P. (1989) *Biochem. J.*, **258**, 817-821.
19. Uribe, S., Rangel, P., Pardo, J. P., and Pereira-da-Silva, L. (1993) *Eur. J. Biochem.*, **217**, 657-660.
20. Williams, R. J. P. (1998) *Biochim. Biophys. Acta*, **1448**, 153-165.
21. Santella, L. (1998) *Biochem. Biophys. Res. Commun.*, **244**, 317-324.
22. Berridge, M. J., Bootman, M. D., and Lipp, P. (1998) *Nature*, **395**, 645-649.
23. Hughes, M. N. (1983) *The Inorganic Chemistry of Biological Processes* [Russian translation], Mir, Moscow, pp. 343-355.
24. Oganessyan, V. Yu., Kurilova, S. A., Vorobyeva, N. N., Nazarova, T. I., Popov, A. N., Lebedev, A. A., Avaeva, S. M., and Harutyunyan, E. H. (1994) *FEBS Lett.*, **348**, 301-304.
25. Josse, J. (1966) *J. Biol. Chem.*, **241**, 1938-1947.
26. Irani, R. R., and Callis, C. P. (1960) *J. Phys. Chem.*, **64**, 1398-1407.
27. Yoshino, M. (1987) *Biochem. J.*, **248**, 815-820.
28. Avaeva, S. M., Rodina, E. V., Kurilova, S. A., Nazarova, T. I., Vorobyeva, N. N., Harutyunyan, E. H., and Oganessyan, V. Yu. (1995) *FEBS Lett.*, **347**, 44-46.
29. Tuominen, V., Heikinheimo, P., Kajander, T., Torkkel, T., Hyytiä, T., Käpylä, J., Lahti, R., Cooperman, B. S., and Goldman, A. (1998) *J. Mol. Biol.*, **284**, 1565-1580.
30. Ting, S. J., and Dunaway-Mariano, D. (1984) *FEBS Lett.*, **165**, 251-253.
31. Inoue, T., Yamada, T., Furuya, E., and Tagawa, K. (1989) *Biochem. J.*, **262**, 965-970.
32. Griffiths, E. J., and Halestrap, A. P. (1993) *Biochem. J.*, **290** (Pt. 2), 489-495.
33. Chen, J., Brevet, A., Fromant, M., Leveque, F., Schmitte, J.-M., Blanquet, S., and Plateau, P. (1990) *J. Bacter.*, **172**, 5686-5689.
34. Cowan, J. A. (1995) *The Biological Chemistry of Magnesium*, VCH Publishers, Inc., New York, pp. 9-11.
35. Spiro, T. G. (1978) in *Inorganic Biochemistry* (Eichhorn, G., ed.) [Russian translation], Vol. 1, Mir, Moscow, pp. 644-650.
36. Welsh, K. M., Jakobyansky, A., Springs, B., and Cooperman, B. S. (1983) *Biochemistry*, **22**, 2243-2248.
37. Avaeva, S. M., Rodina, E. V., Kurilova, S. A., Nazarova, T. I., and Vorobyeva, N. N. (1996) *FEBS Lett.*, **392**, 91-94.
38. Katz, A. K., Glusker, J. P., Beebe, S. A., and Bock, C. W. (1996) *J. Am. Chem. Soc.*, **118**, 5752-5763.
39. Baykov, A. A., Tam-Villosado, J. J., and Avaeva, S. M. (1979) *Biochim. Biophys. Acta*, **569**, 228-238.
40. McCarthy, W. J., Smith, D. M. A., Adamowicz, L., Saint-Martin, H., and Ortega-Blake, I. (1998) *J. Am. Chem. Soc.*, **120**, 6113-6120.
41. Avaeva, S. M., Rodina, E. V., Vorobyeva, N. N., Kurilova, S. A., Nazarova, T. I., Sklyankina, V. A., Oganessyan, V. Yu., Samygina, V. R., and Harutyunyan, E. H. (1998) *Biochemistry (Moscow)*, **63**, 671-684.
42. Kraulis, P. J. (1991) *J. Appl. Crystallogr.*, **24**, 946-950.